Running Head: Right fronto-parietal role in monitoring

RIGHT FRONTO-PARIETAL INVOLVEMENT IN MONITORING SPATIAL TRAJECTORIES

Antonino Vallesi[1,#], Cristiano Crescentini[1]

[1]International School for Advanced Studies (SISSA), Trieste, Italy

[#]Corresponding Author:
Antonino Vallesi
SISSA – Cognitive Neuroscience Sector
Via Bonomea 265, 34136 Trieste, Italy
Phone: +39 040-3787-622
Fax: +39 040-3787-615
E-mail: vallesi@sissa.it

Abstract

This study investigates whether the monitoring role that has been ascribed to the right lateral prefrontal cortex in various cognitive domains also applies to the spatial domain. Specific questions of the study were (i) what kind of spatial contingencies trigger the putative monitoring function of right lateral prefrontal cortex and (ii) which other brain regions are functionally connected to it in monitoring-related conditions. Participants had to track the trajectory of a car moving within a roundabout and detect when the car hits the crash-barrier. Four different trajectories were used with different degrees of regularity and predictability. The results showed that two regions in the right hemisphere, the lateral prefrontal and inferior parietal cortex, were maximally activated and functionally connected when monitoring regular predictable trajectories as compared with unpredictable ones, demonstrating that this fronto-parietal network plays a role in monitoring environmental contingencies that can inform expectancy in a meaningful way.

Keywords: right prefrontal cortex; monitoring; brain asymmetry; expectancy; fronto-parietal network.

The prefrontal cortex has been traditionally thought as the seat of high-level cognitive operations. Mounting evidence shows functional deconstruction within prefrontal cortex. For instance, recent neuropsychological and neuroimaging studies have shown that left and right lateral prefrontal cortices are relatively more associated with computationally different processes such as criterion-setting and monitoring, respectively (e.g., Alexander et al., 2007; Shallice et al., 2008; Stuss et al., 2002; Vallesi, McIntosh, Crescentini, & Stuss, in press; see also Godefroy et al., 1999).

In particular, neuropsychological (Stuss et al., 2005; Triviño et al., 2010; Vallesi et al., 2007a), Transcranial Magnetic Stimulation (TMS; Vallesi et al., 2007b) and neuroimaging (Coull et al., 2000; Vallesi et al., 2009a,b) studies have shown that the right lateral prefrontal cortex is important to monitor temporal probabilities. For instance, it plays a role in optimizing behavior when the probability of a target occurrence increases with elapsing time, such as in the variable foreperiod paradigm (Vallesi et al., 2007a,b; 2009a). In this paradigm, the right dorsolateral prefrontal activation correlates with the RT difference between short and long foreperiods, the latter being associated with a high conditional probability of target occurrence. A monitoring role has been attributed to right lateral prefrontal cortex also in other domains, such as episodic memory retrieval (Henson et al., 1999; Crescentini et al., 2010; Vallesi & Shallice, 2006) and problem solving/reasoning (Reverberi et al., 2005). Although the evidence gathered from different fields and tasks probably advocates a broad monitoring role of right prefrontal cortex, in the context of the present study we use the following operational definition of this process: checking environmental changes that modify the probability of occurrence of critical events, with the goal of optimizing a response to those events.

The aim of the present fMRI study is to test whether not only the right lateral prefrontal cortex but, more extensively, a right fronto-parietal network is involved in monitoring

probabilities in a domain different from the temporal one, namely space. We focus on the spatial domain for the following reasons. First, fronto-parietal regions in the right hemisphere are preferentially involved in temporal and spatial predictions (Beudel et al., 2009). Second, visuospatial orientation of attention has been attributed to right superior temporal (Karnath et al., 2004) and inferior parietal regions, such as the supramarginal (Vallar & Perani, 1986) and angular gyri (Mort et al., 2003) in works on unilateral spatial neglect and neuroimaging studies on healthy participants (Corbetta & Shulman, 2002; Galati et al., 2000). A recent TMS study on healthy individuals performing line bisection judgments attributed a more important role to the right supramarginal gyrus than to the right superior temporal or angular gyri (Oliveri & Vallar, 2009). Moreover, lateral prefrontal and parietal regions, which subserve spatially guided behaviour, have many common efferent projections in the brain (Selemon & Goldman-Rakic, 1988) and show reciprocal effective connectivity through superior and longitudinal fasciculi. These fiber tracts, in turn, if lesioned in the right hemisphere, may also produce neglect symptoms (Doricchi & Tomaiuolo, 2003; Thiebaut de Schotten et al., 2005).

We therefore expected functional connectivity between right prefrontal and parietal regions, specifically when monitoring of spatial contingencies is advantageous for the behaviour. Therefore, a second aim of the study was to assess whether the right fronto-parietal network is specifically involved in monitoring spatial trajectories that are informative about the probability of occurrence of a critical event, rather than in monitoring spatial contexts in general.

To test this hypothesis we designed a visuo-spatial tracking task, in which participants were asked to play the role of ‘traffic agents’ that had to constantly monitor the behaviour of an inattentive driver. They had to detect when the driver’s car moving within a roundabout hit either the external or the internal crash-barrier (see Methods and Figure 1 for details). During

non-baseline periods, the car moved following one of four different types of spatial trajectories with different degrees of regularity and predictability. In a regular predictable trajectory, for instance, the car progressively approached either the internal or the external barrier until it actually struck the barrier. Predicting the occurrence of an accident by monitoring the spatial trajectory was impossible in the other trajectory types (regular unpredictable, random and zig-zag).

Our main prediction was that a right fronto-parietal network would be more engaged and functionally coupled throughout the highly probabilistic (i.e., regular predictable) trajectories than during the other kinds of trajectories. The latter trajectories were expected to activate the right fronto-parietal network gradually to a less extent, with minimal activation associated to the zig-zag trajectory. In this condition, monitoring processes would in fact be of no help, since approaching a crash-barrier was often misleading because the car then turned back towards the centre of the road a variable number of times before hitting one of the barriers.

----*Insert Figure 1 about here*----

Methods

Participants

Eighteen healthy participants (9 females; mean age: 28 years, range: 22-37) were recruited in this study after signing an informed consent for this study, which was previously approved by “La Nostra Famiglia” ethical committee. All participants had normal or corrected-to-normal vision, and were right-handed, as assessed with the Edinburgh Handedness Inventory (Oldfield, 1971; average score: 83, range: 55-100). None reported any history of psychiatric or neurological disorders. Participants received 25 Euros for their time.

Experimental material and design

Stimuli were green and red circles symbolizing a car which moved on a constantly displayed roundabout according to different trajectories. The apparent movement of the cars was obtained with the circle changing position every 500 ms. Each trial began with a baseline trajectory. A green circle (car) started to move either clockwise or counter-clockwise from a position in the centre of the road and occupied a random number (4-15) of subsequent positions always in the centre of the road. During the baseline trajectory, a picture with sunny weather was constantly shown in the middle of the roundabout. Participants were told that no accident would occur with sunny weather. The start of each test trajectory was marked (i) by a change in the central picture, which now showed a rainy cloud, and at the same time (ii) by a change in the color of the car, which turned red (see Figure 1). Participants were told that these changes indicated a high probability of accident occurrence (5/6). The red car advanced in one direction by occupying a random number of positions (8-12, one every 500 ms) following the 4 different types of trajectories described in details in the introduction: regular predictable, regular unpredictable, random and a curved version of a zig-zag trajectory. An analytical description of each part of the background roundabout and each type of trajectory used in the experiment is presented in Table 1. Some illustrative examples of trajectories can be appreciated in Figure 2.

-----Insert Table 1 about here-----

----Insert Figure 2 about here----

For each of the 4 trajectories, a catch trial occurred1/6 of the time: the car did not hit any crash-barrier but simply disappeared after the last position (12^{th}) occupied. Catch trials were included to maintain a constant conditional probability of occurrence for the critical event

until the last position and reduce foreperiod-like phenomena (Correa, Lupiañez, & Tudela, 2006; Vallesi et al., 2009a). A blank screen of 2000 ms followed the target event (car hitting a crash-barrier) in non-catch trials or the last stimulus presentation in catch trials.

Participants had to detect when the car hit the internal or external crash-barrier by pressing a button with the right index finger. The type of accident (crash on the internal vs. external barrier) varied randomly across trials. It was impossible to predict an accident on the basis of the epoch duration (6 random durations). Responses were collected with a deadline of 2000 ms after the accident onset.

There were 4 runs in total. For each run, a first familiarization phase with 4 baseline-test trajectory cycles preceded the real test, which consisted of 48 baseline-test cycles. The driving direction (clockwise, counterclockwise) was different on even and odd runs and the starting direction was counterbalanced between participants. Participants saw the visual scene through MRI-compatible goggles mounted on the head-coil that were regulated according to their feedback at the beginning of the MRI session.

Behavioral Data Analysis. RTs shorter than 100 ms (0.087%) and responses during catch trials (0.09%) were rare and were excluded from further analyses. Misses (which included responses longer than 2000) ms were analyzed using a non-parametric Friedman ANOVA. A one-way repeated-measures ANOVA was used to analyze RTs to correct trials, with trajectory type as the within-subjects factor (4 levels).

Acquisition and Pre-processing of fMRI data. Scanning was performed at the S. Maria della Misericordia Hospital in Udine on a 3T Achieva Philips whole-body scanner with an 8-channel head coil. Head movements were minimised through apposite cushioning. Functional volumes were obtained using a whole head T2*-weighted echo-planar image (EPI) sequence

(repetition time, TR: 2 sec; echo time, TE: 35 ms; 34 transverse axial slices with interleaved acquisition; flip angle: 90; 3.59x3.59x4 mm voxel size; field of view, FOV: 23 cm, acquisition matrix: 64x64; SENSE factors: 2 in anterior-posterior direction). Anatomical images (TR/TE: 8.2/3.7, 190 transverse axial slices; flip angle: 8; 1 mm^3 voxel size; FOV = 24 cm; acquisition matrix: 240x240; no SENSE factors) were acquired after the first 2 functional runs. Stimulus presentation and response collection were controlled using Presentation software (www.neurobs.com) and delivered within the scanner by means of MR-compatible goggles mounted on the coil. Manual responses were recorded using a response pad.

The fMRI data pre-processing and statistical analyses were performed using SPM8 (www.fil.ion.ucl.ac.uk/SPM). Functional images were spatially realigned and unwarped to compensate for participants' head movements during the experiment using a 4^{th} degree B-Spline interpolation. For normalization, a transformation matrix between the mean image of realigned volumes and a standard functional Montreal Neurological Institute (MNI) template (EPI.nii) was generated with a 4^{th} degree B-spline algorithm and applied to re-slice volumes with a 2 mm^3 voxel-size. The functional images were then spatially smoothed with an 8 mm full-width-at-half-maximum Gaussian filter to reduce residual inter-individual anatomical variability.

fMRI statistical analysis. For each participant, first-level analysis was performed using General Linear Model. The data were modelled with nine conditions (the four trajectories in non-catch trials, the four trajectories in catch/no-response trials, and baseline), each modelled as an epoch convolved with a canonical hemodynamic response function. The duration of each epoch corresponded to the duration of each trajectory. We used brief epochs instead of single events since the former would better capture activity that is sustained throughout the

processing of a given trajectory (Grinband et al., 2008). Estimates of head movements from realignment were included in the matrix as six additional regressors of no interest. Slow signal drifts were removed using a 128 sec high-pass filter. For each participant, four t-contrasts were extracted comprising the 4 trajectory types in non-catch trials in which the subjects responded within the 2 sec deadline. The SPM group maps were generated with a random-effects model within SPM8 using the individual contrast maps. A 'full factorial' ANOVA model was used comprising one factor with 4 levels (trajectory types). An F-contrast of the main effect of trajectory was first extracted. Then, 2 t-contrasts of interest were also extracted: (i) A linear contrast with the following weights: regular predictable (+3), regular unpredictable (+1), random unpredictable (-1), zig-zag (-3); (ii) a simple contrast between the regular predictable (+1) and the zig-zag (-1) trajectories. Other contrasts extracted included: zig-zag vs. the other conditions, to test for the neural source of the behavioural advantage in this condition; zig-zag and regular predictable vs. random and regular unpredictable, to test which regions were associated with the conditions with shorter RTs; and the opposite contrast of random and regular unpredictable vs. zig-zag and regular predictable trajectories, to test which regions were associated with the conditions with longer RTs. The statistical significance was generally set at cluster-wise $p < 0.05$, corrected for multiple comparisons using False Discovery Rate, unless stated otherwise.

The MNI coordinates of the peak voxel within each cluster were transformed into Talairach space using M. Brett's transformation (http://www.mrccbu.cam.ac.uk/Umaging/mnispace.html) and inputted into Talairach Daemon (Lancaster et al. 2000) to find the likely Brodmann areas (BA).

Psychophysiological Interaction (PPI). PPI (Friston et al., 1997) computes functional connectivity between the time-series of a seed voxel and the time-series of all other voxels.

The time-series data of the peak voxel in right lateral prefrontal cortex within the contrast between regular predictable and zig-zag trajectories [MNI coordinates: 46, 38, 10] were extracted, temporally filtered and mean corrected as in conventional SPM analysis. When this voxel did not show activation at $p \leq .05$, the nearest voxel passing this threshold was used. Bayesian estimation was used to deconvolve the time-series of the BOLD signal and generate the time-series of the neuronal signal for the seed voxel. Three vectors were created and used as regressors in the PPI analysis: one vector (the Y regressor) consisting of the seed voxel time-course (the physiological variable), a second vector (the P regressor) representing the contrast for the main effect of regular predictable vs. zig-zag unpredictable trajectories (the psychological variable), and a third vector (the PPI regressor) representing the interaction between the psychological context and the seed voxel. These regressors were forward-convolved with the canonical hemodynamic response function (HRF), and then entered into the regression model along with vectors for session effects. Model estimation was performed for each participant and the resulting images of contrast estimates for the interaction term showed areas with significant differential connectivity to the seed voxel due to context manipulations. The interaction images of each participant were entered into a one-sample t-test to assess group effects.

Results

Behavioral results. Speed differed across conditions [$F(3,51)=102.8$, $p<0.0001$, see Table 2]. RTs were shorter for regular predictable and cyclical unpredictable (zig-zag) trajectories than for random and regular unpredictable ones (for both, Tukey test $p<.001$). No difference was observed between regular predictable and cyclical unpredictable trajectories (Tukey test $p=.96$) or between regular unpredictable and random ones (Tukey test $p=.85$).

Missed targets did not differ significantly across conditions [Friedman ANOVA Chi Sqr. (N: 18, df: 3)=1.36, p=.71].

-----Insert Table 2 about here-----

fMRI results. A first F-contrast testing for the main effect of the trajectory type showed a significant cluster in the bilateral cuneus (BA 17, 18). When the threshold was increased at an uncorrected p-value of 0.001 at the voxel-level, and a minimum cluster size of 20 voxels, there was also additional activation in right frontal (BA 46, 47) and parietal (BA 40) areas (see Table 3). More detailed contrasts were run to test which condition was associated with the activation of each of these regions.

A hypothesis-driven contrast between regular predictable and cyclical unpredictable conditions showed activation in right lateral prefrontal and parietal regions (Table 3). We then extracted the beta parameter estimates for each of the four conditions and observed (Figure 3B) that the signal was highest for the regular predictable trajectory, followed by the regular unpredictable and then the random trajectory. Finally, the lowest activation was for the cyclical unpredictable trajectory. A linear contrast statistically corroborated this pattern in both right parietal and frontal regions (Table 3 and Figure 3A).

----Insert Figure 3 about here----

Since the RTs to the cyclical unpredictable condition were as short as in the regular predictable one and significantly shorter than in the other two conditions (random and regular unpredictable), we also investigated which brain regions might drive this behavioral advantage with a contrast between the cyclical unpredictable condition and all the rest. No

cluster survived correction for multiple comparisons in this contrasts. We therefore lowered the single-voxel threshold as a $p < .01$ (voxel size≥20), uncorrected, to explore whether there were some brain regions that survived this more liberal criterion. Three regions survived this threshold, namely the lateral portion of the left middle occipital gyrus (BA 18), posterior cingulate (BA 23) and frontal pole (BA 10). However, since the behavioral advantage was also observed in the regular predictable condition, a further contrast was performed comparing the zig-zag and the regular predictable trajectories against the random and regular unpredictable ones. This contrast, when the significance threshold was lowered at $p<.01$ (cluster size≥20) generated activations in the lateral portion of middle and inferior occipital gyrus bilaterally (BA 18) and left putamen. The opposite contrast, instead, generated a significant cluster in the medial visual cortex approximately corresponding to the foveal region (BA 17, 18), suggesting a critical role of the primary visual cortex in tracking spatial trajectories in which forecasting of the critical event (and optimal response preparation) was not possible because of randomness or uninformative regularity.

-----*Insert Table 3 about here*-----

PPI results. A Psychophysiological interaction (PPI) analysis was run to assess increases in coupling between the main right lateral prefrontal cluster and other brain regions driven by meaningful task contexts (regular predictable vs. zig-zag unpredictable trajectory contrast). This analysis produced significant activations in various regions (see Table 4 and Figure 4), including right inferior (BA 44) and middle frontal (BA 10) gyri, right cerebellum, bilateral superior frontal and precentral gyrus (BA 6), probably including the frontal eye fields (Paus, 1996) although slightly more dorsal than the location conventionally reported as the frontal eye fields, and middle and superior occipital cortex (BA 7, 18, 19, 37). Some of the clusters

functionally connected with the right prefrontal node almost certainly play a role related to the specific perceptual and motor demands of the task. In particular, the functional connectivity with foveal and para-foveal visual regions was probably useful to continuously gather bottom-up information about the position of the moving dot (imaginary car); working in concert with associative occipito-parietal visual regions might also be related to the perceptual nature of the visuo-spatial tracking task; the connectivity with right cerebellum, left pre- and post-central gyrus and premotor regions is most probably related to the optimal preparation of a right motor response to target events (i.e., car accident) under predictable conditions. Moreover, the right inferior parietal and post-central gyrus (BA 40, 2) were also functionally connected with the right frontal seed in a cluster close to (albeit not exactly corresponding to) the parietal area activated in the linear contrast and in the regular predictable vs. zig-zag contrast of the main SPM analysis.

-----Insert Table 4 about here-----

----Insert Figure 4 about here----

Discussion

The aim of the present fMRI study was twofold: to investigate whether the right lateral prefrontal cortex is involved in monitoring spatial contingencies and whether this involvement is specific of contexts which convey probabilistic information about the occurrence of critical events. The results showed that indeed right lateral prefrontal cortex was maximally activated when participants needed to track regular trajectories that were highly predictable about the occurrence of a critical event. This region was less strongly activated with regular trajectories which were neither spatially predictable nor misleading, while it was even less activated with random spatial trajectories. Finally, right lateral

prefrontal cortex was least activated with zig-zag trajectories that were regular but misleading, since approaching the crash-barrier was not diagnostic of the occurrence of an accident in this context.

Another region in the right inferior parietal lobule corresponding to the supramarginal gyrus (BA 40) was also activated with a pattern similar to that of the right prefrontal region. This finding corroborates other studies showing that the right supramarginal gyrus plays a key-role in visuo-spatial judgments (Fink et al., 2003; Oliveri & Vallar, 2009; Vallar & Perani, 1986) and strategic orienting of spatial attention (Perry & Zeki, 2000). On the other hand, we did not find evidence of an involvement of right angular gyrus or superior temporal regions in our task conditions, despite others have stressed their role in spatial attention (e.g., Karnath et al., 2004; Mort et al., 2003).

The fronto-parietal co-activation has also been observed in the literature on spatial attention (e.g., Corbetta & Shulman, 2002). These regions are likely to be effectively connected through fronto-parietal pathways (e.g., Bartolomeo, Thiebaut de Schotten & Doricchi, 2007), such as the superior occipito-frontal fasciculus, which plays an important role in spatial awareness, as demonstrated with intra-operative electrical stimulation in humans (Thiebaut de Schotten et al., 2005).

We found a dissociation between the behavioural measure and the activation pattern: although the right fronto-parietal network was maximally activated during regular predictable trajectories and minimally during zig-zag unpredictable ones, both these conditions produced the lowest RTs with respect to the other two types of trajectory (random and regular unpredictable). This pattern increases our confidence that the right fronto-parietal activations observed in our study are not simply driven by different levels of general difficulty in tracking the different trajectories but subserve a monitoring role in the spatial domain, which is critical for regular predictable trajectories only.

The next question was whether the fronto-parietal regions, which are known to be effectively connected through fiber bundles (e.g., Thiebaut de Schotten et al., 2005), besides from being maximally co-activated during regular predictable trajectories, were also part of a functional network subtending monitoring of meaningful spatial information. We investigated functional connectivity in tracking the regular predictable trajectory (as opposed to tracking the zig-zag one) by implementing a Psycho-Physiological Interaction in SPM with the right lateral prefrontal peak voxel as the seed. This analysis unveiled a network functionally connected to the right lateral prefrontal cortex, mainly including right-lateralized regions (especially in the prefrontal cortex) but also bilateral parietal regions, the dorsal visual stream and motor-related regions important for planning ocular and hand movements, which was cohesively activated when tracking regular predictable trajectories as compared to tracking zig-zag unpredictable ones. Thus, the speed advantage in the regular predictable trajectory is probably explained by the monitoring role of fronto-parietal networks activated in this context.

The behavioural advantage during the zig-zag trajectory is instead unlikely to be explained in this way. This advantage is probably due to a perceptual counterpart to the well-known motor advantage in producing rhythmic movements, which requires only a subset of regions required for more discrete movements (Schaal et al., 2004). The zig-zag trajectory indeed showed activation in the bilateral middle occipital gyrus, which was common with the regular predictable trajectory. The difference with this condition was that this occipital cluster was functionally connected to the right frontal one in the regular predictable context but not in the zig-zag one, suggesting a bottom-up influence on behavioural preparation in the latter case. This occipital cluster in BA 18 was more lateral than that differentially more activated for unpredictable random and regular trajectories, which probably corresponded to the foveal primary and secondary occipital cortex (BA 17, 18). The zig-zag condition also produced an

additional selective activation in the posterior cingulate and frontal pole (BA 10), compatible with an involvement of the default network (Raichle et al., 2001) in this easy-to-track condition. The frontal pole (BA 10) involvement in this condition is also compatible with the gateway hypothesis (Gilbert et al., 2005): this region might sustain a bottom-up visual tracking strategy against a less appropriate top-down monitoring strategy based on the right fronto-parietal network.

Monitoring was defined here as the process which constantly checks the probability of occurrence of a critical event, which the present study examined in the context of a visuo-spatial task. The present findings, especially those concerning the right lateral prefrontal cortex, can possibly be generalized beyond the spatial domain, as a monitoring role has already been attributed to this region in other domains such as timing (e.g., Coull et al., 2000; Vallesi et al., 2007a,b). However, this hypothesis still awaits confirmation by future research studies, in which monitoring will be investigated in multiple domains using within-subject designs. Those studies will also clarify how the functional connectivity of right lateral prefrontal cortex with the rest of the brain evolves according to the different domains and contexts used.

In conclusion, the present study showed that a right prefrontal region functionally connected to a fronto-parietal and occipital network is important to monitor spatial trajectories that are highly informative about the occurrence of critical events, generalizing its monitoring role already shown in other cognitive contexts to the spatial domain.

References

Alexander, M.P., Stuss, D.T., Picton, T., Shallice, T., & Gillingham, S. (2007). Regional frontal injuries cause distinct impairments in cognitive control. *Neurology, 68,* 1515-1523.

Bartolomeo, P., Thiebaut de Schotten, M., & Doricchi, F. (2007). Left unilateral neglect as a disconnection syndrome. *Cereb Cortex, 17,* 2479–90.

Beudel, M., Renken, R., Leenders, K.L., & de Jong, B.M. (2009). Cerebral representations of space and time. *Neuroimage, 44,* 1032-1040.

Corbetta, M. & Shulman, G.L. (2002). Control of goal-directed and stimulus-driven attention in the brain. *Nat.Rev.Neurosci., 3,* 201-215.

Correa, A., Lupiañez, J., & Tudela, P. (2006). The attentional mechanism of temporal orienting: determinants and attributes. *Exp Brain Res., 169,* 58-68.

Coull, J.T., Frith, C.D., Buchel, C., & Nobre, A.C. (2000). Orienting attention in time: behavioural and neuroanatomical distinction between exogenous and endogenous shifts. *Neuropsychologia, 38,* 808-819.

Crescentini, C., Shallice, T., Del Missier, F., & Macaluso, E. (2010). Neural correlates of episodic retrieval: An fMRI study of the part-list cueing effect. Neuroimage, 50, 678-692.

Thiebaut de Schotten, M., Urbanski, M., Duffau, H., Volle, E., Levy, R., Dubois, B. , Bartolomeo, P. (2005). Direct evidence for a parietal-frontal pathway subserving spatial awareness in humans. *Science, 309,* 2226-2228.

Doricchi, F., & Tomaiuolo, F. (2003). The anatomy of neglect without hemianopia: a key role for parietal-frontal disconnection? *Neuroreport, 14,* 2239–43.

Henson, R.N., Rugg, M.D., Shallice, T., Josephs, O., Dolan, R.J., 1999a. Recollection and familiarity in recognition memory: an event-related functional magnetic resonance imaging study. J. Neurosci. 19, 3962–3972.

Fink, G.R., Marshall, J.C.,Weiss, P.H., Stephan, T., Grefkes, C., Shah, N.J., et al. (2003). Performing allocentric visuospatial judgments with induced distortion of the egocentric reference frame: An fMRI study with clinical implications. *Neuroimage, 20,* 1505-1517.

Friston, K.J., Buechel, C., Fink, G.R., Morris, J., Rolls, E., & Dolan, R.J. (1997). Psychophysiological and modulatory interactions in neuroimaging. *Neuroimage, 6,* 218-229.

Galati, G., Lobel, E., Vallar, G., Berthoz, A., Pizzamiglio, L., & Le Bihan, D. (2000). The neural basis of egocentric and allocentric coding of space in humans: A functional magnetic resonance study. *Experimental Brain Research, 133,* 156-164.

Gilbert S.J., Frith C.D., & Burgess, P.W. (2005). Involvement of rostral prefrontal cortex in selection between stimulus-oriented and stimulus-independent thought. *European Journal of Neuroscience, 21,* 1423-1431.

Grinband, J., Wager, T.D., Lindquist, M., Ferrera, V.P., & Hirsch, J. (2008). Detection of time-varying signals in event-related fMRI designs. *Neuroimage, 43,* 509-520.

Godefroy, O., Cabaret, M., Petit-Chenal, V., Pruvo, J.-P. & Rousseaux, M. (1999) Control functions of the frontal lobes: Modularity of the central-supervisory system? *Cortex, 35,* 1-20.

Karnath, H.O., Fruhmann, B.M., Kuker, W., & Rorden, C. (2004). The anatomy of spatial neglect based on voxelwise statistical analysis: a study of 140 patients. *Cereb.Cortex, 14,* 1164-1172.

Lancaster, J.L., Woldorff, M.G., Parsons, L.M., Liotti, M., Freitas, C.S., Rainey, L., Kochunov, P.V., Nickerson, D., Mikiten, S.A., Fox, P.T. (2000). Automated Talairach atlas labels for functional brain mapping. *Hum Brain Mapp, 10,* 120-31.

Mort, D.J., Malhotra, P., Mannan, S.K., Rorden, C., Pambakian, A., Kennard, C. et al. (2003). The anatomy of visual neglect. *Brain, 126,* 1986-1997.

Oldfield, R.C. (1971). The assessment and analysis of handedness: the Edinburgh inventory. *Neuropsychologia, 9,* 97-113.

Oliveri, M., & Vallar, G. (2009). Parietal versus temporal lobe components in spatial cognition: Setting the mid-point of a horizontal line. *Journal of Neuropsychology, 3,* 201-211.

Paus, T. (1996). Location and function of the human frontal eye-field: a selective review. *Neuropsychologia, 34,* 475-483.

Perry, R.J., & Zeki, S. (2000). The neurology of saccades and covert shifts in spatial attention: An event-related fMRI study. *Brain, 123,* 2273-2288.

Raichle, M.E., MacLeod, A.M., Snyder, A.Z., Powers, W.J., Gusnard, D.A., & Shulman, G.L. (2001). A default mode of brain function. *Proc.Natl.Acad.Sci.U.S.A, 98,* 676-682.

Reverberi, C., Lavaroni, A., Gigli, G. L., Skrap, M., & Shallice, T. (2005). Specific impairments of rule induction in different frontal lobe subgroups. Neuropsychologia, 43, 460-472.

Schaal, S., Sternad, D., Osu, R., & Kawato, M. (2004). Rhythmic arm movement is not discrete. *Nat.Neurosci., 7,* 1136-1143.

Selemon, L.D. & Goldman-Rakic, P.S. (1988). Common cortica and subcwork subserving spatial guided behaviorortical targets of the dorsal prefrontal and posterior parietal cortices in the Rhesus monkey: evidence for a distributed neural net. *Journal of Neuroscience, 8,* 4049-4068.

Shallice, T., Stuss, D.T., Alexander, M.P., Picton, T.W., & Derkzen, D. (2008). The multiple dimensions of sustained attention. *Cortex, 44,* 794-805.

Stuss, D.T., Alexander, M.P., Shallice, T., Picton, T.W., Binns, M.A., Macdonald, R. Borowiec, A., Katz, D.I. (2005). Multiple frontal systems controlling response speed. *Neuropsychologia, 43,* 396-417.

Stuss, D.T., Binns, M.A., Murphy, K.J., & Alexander, M.P. (2002). Dissociations within the anterior attentional system: effects of task complexity and irrelevant information on reaction time speed and accuracy. *Neuropsychology, 16,* 500-513.

Triviño, M., Correa, A., Arnedo, M., & Lupiañez, J. (2010). Temporal orienting deficit after prefrontal damage. *Brain, 133,* 1173-1185.

Vallar, G. & Perani, D. (1986). The anatomy of unilateral neglect after right-hemisphere stroke lesions. A clinical/CT-scan correlation study in man. *Neuropsychologia, 24,* 609-622.

Vallesi A., McIntosh A.R., Crescentini C., Stuss D.T. (in press). FMRI investigation of speed-accuracy strategy switching. Human Brain Mapping. Date of Acceptance: 3-3-2011.

Vallesi, A., McIntosh, A.R., Shallice, T., & Stuss, D.T. (2009a). When time shapes behavior: FMRI evidence of brain correlates of temporal monitoring. *J.Cogn Neurosci., 21,* 1116-1126.

Vallesi A., McIntosh A.R., Stuss D.T. (2009b). Temporal preparation in aging: a functional MRI study. *Neuropsychologia, 47,* 2876–2881.

Vallesi, A., Mussoni, A., Mondani, M., Budai, R., Skrap, M., & Shallice, T. (2007a). The neural basis of temporal preparation: Insights from brain tumor patients. *Neuropsychologia, 45,* 2755-2763.

Vallesi, A., Shallice, T., & Walsh, V. (2007b). Role of the prefrontal cortex in the foreperiod effect: TMS evidence for dual mechanisms in temporal preparation. *Cereb.Cortex, 17,* 466-474.

Vallesi, A. & Shallice, T. (2006). Prefrontal involvement in source memory: an electrophysiological investigation of accounts concerning confidence and accuracy. *Brain Res., 1124,* 111-125.

Acknowledgements

This research was partially supported by a grant from Regione Autonoma Friuli Venezia Giulia to SISSA. The authors thank the following people for their kind support in facilitating this study: Paolo Brambilla (IRCSS Medea-Nostra Famiglia and DSMSC Università di Udine); Shima Seyed-Allaei (SISSA, Trieste); Serena D'Agostini, Marta Maieron and Antonio Margiotta (Azienda Ospedaliero-Universitaria S. Maria della Misericordia, Udine).

Table 1. Parameters (in pixels) describing parts of the background frame (roundabout) and types of trajectory used in the experiment (see Figure 2 for a graphical illustration).

Inner Circle [#1 in Figure 2]

Phi	X center	Y center	Diameter
0	0	0	181

Outer Circle [#2 in Figure 2]

Phi	X center	Y center	Diameter
0	0	0	546

Middle circle (but parts of it can also describe baseline and regular unpredictable trajectories) [#3 in Figure 2]

Phi	X center	Y center	Diameter
0	0	0	364

Regular predictable trajectory (towards the inner crash-barrier) [#4 in Figure 2]

Phi	X center	Y center	Long axis (ellipse)	Short axis (ellipse)
0	-36	-15	255	231

Regular predictable trajectory (towards the outer crash-barrier) [#5 in Figure 2]

Phi	X center	Y center	Long axis	Short axis
0	-61	6	554	489

Curved version of a zig-zag trajectory: each curve can be fitted by a second-degree polynomial [#6 in Figure 2]

y = x^2 - 2 x + 63 (first 5 points in the illustrative Figure 2, top right)

y = x^2 + 1 x -72 (last 6 points in the illustrative Figure 2, top right)

Random Trajectory (#7 in Figure 2)

Parameters = N/A. No function fits a random trajectory by definition

Table 2. Mean RTs for correct target identification and percentage of misses according to trajectory type. The standard errors of the mean are shown in brackets.

	Regular Predictable	Cyclical Unpredictable (Zig-Zag)	Random Unpredictable	Regular Unpredictable
RTs (ms)	362 (18.0)	366 (16.1)	466 (15.9)	473 (16.0)
Misses (%)	2.2 (0.8)	1.1 (0.6)	1.0 (0.4)	1.9 (1.0)

Table 3. Significant cluster activations in SPM analyses. BA: Brodmann area.

Anatomical Localization	BA	MNI coordinates			Peak p-corr.	Peak Z-value	Voxels per Cluster
		X	y	z			
F-Contrast							
R. Lingual Gyrus	17	6	-88	-4	0.001	5.53	1075
2nd peak R. Cuneus	18	14	-98	6	0.005	5.14	
3rd peak L. Cuneus	18	-8	-102	6	0.183	3.99	
R. Inf. Frontal Gyrus**	47	44	18	-8	0.141	4.25	40
R. Inf. Parietal L.**	40	60	-40	42	0.183	4.04	62
L. Middle Occipital G.**	18	-18	-86	-10	0.183	3.99	181
2nd peak Left Lingual G.**	18	-26	-80	-8	0.433	3.56	
R. Inf. Frontal Gyrus**	46	46	38	10	0.5	3.48	27
Linear Contrast Analysis							
Anatomical Localization	**BA**	**MNI coordinates**			**Cluster p-corr.**	**Peak Z-value**	**Voxels per Cluster**
		X	**y**	**z**			
R. Inf. Frontal Gyrus	47	44	18	-8	0.031	4.7	182
R. Inf./mid. Frontal G.	46	46	38	10	0.026	4.25	228
2nd peak Mid. Frontal G.	47	46	46	-6		3.58	
R. Inf. Parietal Lobule	40	60	-40	42	0.032	4.25	159
Regular predictable vs. Cyclical unpredictable							
R. Inf. Parietal Lobule	40	60	-38	42	0.035	4.2	153
R. Inf. Frontal Gyrus	46	46	38	10	0.035	4.16	148
Cyclical unpredictable vs. All							
L. Mid. Occipital Gyrus*	18	-22	-104	4	0.916	2.99	44
L. Sup. Frontal Gyrus*	10	-8	60	-8	0.916	2.82	22
L. Posterior Cingulate*	23	-6	-62	16	0.916	2.66	29
Cyclical unpredictable & Regular Predictable (short RTs) vs. the rest (long RTs)							
L. Mid. Occipital G.*	18	-26	-104	-6	0.341	3.02	99
2nd peak Mid. Occip. G.*	18	-32	-94	-8		2.78	
R. Inf. Occipital G.*	18	34	-90	-10	0.341	2.96	113
2nd peak Mid. Occip. G.*	18	42	-90	-4		2.8	
3rd peak Inf. Occip. G.*	18	30	-98	-12		2.38	
L. Lentiform Nucleus*		-22	10	-6	0.341	2.77	77
2nd peak Parahippoc G.*		-26	2	-12		2.7	
Random & Regular Unpredictable (long RTs) vs. the rest (short RTs)							
L. Middle Occipital G.	18	-10	-100	14	<.0001	4.27	1075
2nd peak R. Lingual G.	17	4	-88	-2		4.26	
3rd peak R. Cuneus	17	14	-98	12		4.06	

Some clusters did not survive correction for multiple comparisons but were significant at an uncorrected p=.001, voxel size≥20 (**); or p=.01, voxel size≥20 (*).

Table 4. Significant cluster activations in the Psychophysiological Interaction analysis.

Anatomical Localization	BA	MNI coordinates			Cluster p-corr.	Peak Z-value	Voxels per Cluster
		X	y	z			
L. Sup. Frontal G.	6	-28	-10	70	< .0001	5.32	1258
2nd peak L. Precentral G.	6	-44	-4	48		4.52	
3rd peak L. Postcentral G.	3	-34	-38	64		4.45	
R. Middle Frontal G.	6	32	-2	48	< .0001	5.02	778
2nd peak R. Inf. Frontal G.	44	56	6	22		4.99	
3rd peak R. Mid. Frontal G.	6	42	2	48		4.74	
R. Precuneous	7	32	-50	52	< .0001	4.66	3023
2nd peak R. Inf. Temp. G.	19	48	-58	-8		4.52	
3rd peak R. Mid. Occip G.	19	54	-64	-8		4.49	
R. Precentral G.	44	56	14	6	0.024	4.64	117
L. Middle Occip. G.	37	-56	-72	0	< .0001	4.49	815
2nd peak L. Inf. Temp. G.	19	-48	-74	-6		4.29	
3rd peak L. Fusiform G.	19	-44	-70	-16		4.16	
R. Sup. Frontal G.	6	10	-4	70	0.049	4.46	91
2nd peak R. Sup. Front. G.	6	14	10	70		3.4	
L. Sup. Occip. G.	19	-34	-90	20	< .0001	4.45	345
2nd peak L. Mid. Occip G.	18	-32	-96	6		4.11	
3rd peak L. Mid. Occip. G.	18	-30	-100	-6		3.35	
R. Declive	*	32	-66	-30	0.005	4.29	177
2nd peak R. Declive	*	24	-72	-30		3.67	
3rd peak R. Culmen	*	30	-52	-32		3.23	
R. Inf. Parietal L.	40	46	-36	36	0.003	4.18	199
2nd peak R. Postcentral G.	2	52	-26	40		3.69	
3rd peak R. Postcentral G.	2	56	-32	44		3.36	
L. Substania Nigra	*	-8	-20	-16	0.011	4.17	143
2nd peak L. Red Nucleus	*	-4	-24	-4		4	
3rd peak L. Substania Nigra	*	-8	-12	-10		3.8	
L. Postcentral G.	2	-42	-30	36	0.002	4.15	219
2nd peak L. Inf. Parietal L.	40	-56	-26	32		3.8	
3rd peak L. Postcentral G.	2	-52	-28	44		3.8	
R. Middle Frontal G.	10	36	38	24	0.049	4.14	89
2nd peak R. Mid. Frontal G.	10	36	46	28		3.78	
3rd peak R. Sup. Frontal G.	10	26	48	26		3.28	
R. Sup. Frontal G.	6	4	12	56	0.008	3.78	157
R. Declive	*	0	-60	-24	0.024	3.66	114
2nd peak R. Dentate	*	14	-56	-26		3.57	

Figure Captions

Figure 1. A representation of the inattentive driver task. The example shows a regular predictable trajectory (active period) with a critical event occurring at the end of the trajectory (car hitting the external crash-barrier). Each circle represents a subsequent position occupied by the circle (car) every 500 ms.

Figure 2. Illustration of the stimuli used. Each number in the four roundabouts represents a specific part of the roundabout or an example of a trajectory (analytically described in Table 4): 1. Inner Circle; 2. Outer Circle; 3. Middle circle and (partly) baseline and regular unpredictable trajectories; 4. Regular predictable trajectory (towards the inner crash barrier); 5. Regular predictable trajectory (towards the outer crash barrier); 6. Curved version of a zig-zag trajectory; 7. Random trajectory.

Figure 3. Panel A: Significant clusters activated in the following linear contrast: regular predictable (+3), regular unpredictable (+1), random (-1) and zig-zag (-3) trajectories. Panel B: Beta parameter estimates (in arbitrary units, ± 90% confidence interval) in the right inferior/middle frontal peak voxel for each of the 4 conditions.

Figure 4. Significant clusters activated in the psycho-physiological interaction analysis with the right middle frontal voxel used as the seed voxel (physiological variable) and the contrast between regular predictable and zig-zag trajectories as the psychological context.

Fig. 1

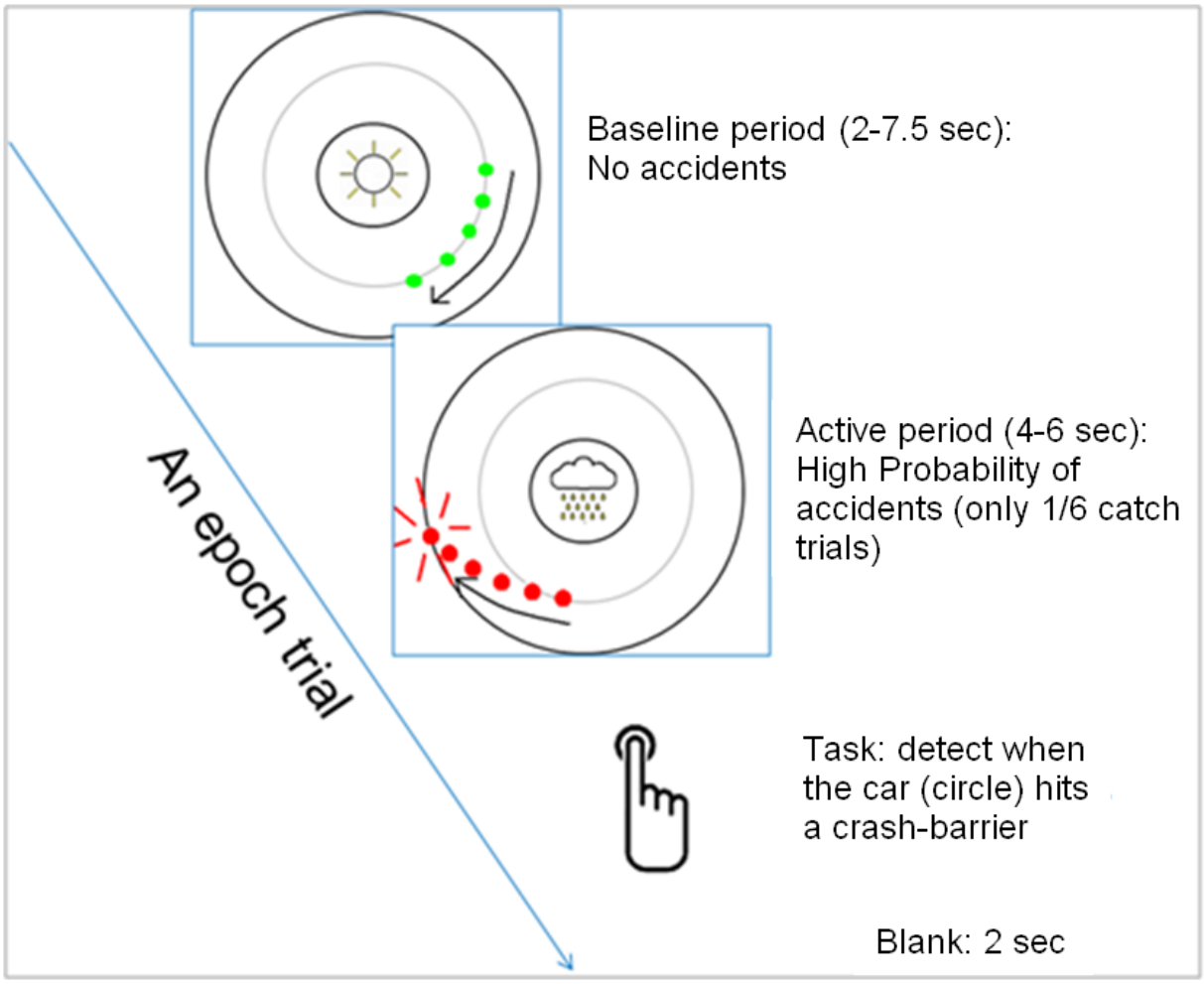
Baseline period (2-7.5 sec):
No accidents
Active period (4-6 sec):
High Probability of
accidents (only 1/6 catch
trials)
An epoch trial
Task: detect when
the car (circle) hits
a crash-barrier
Blank: 2 sec

Fig. 2

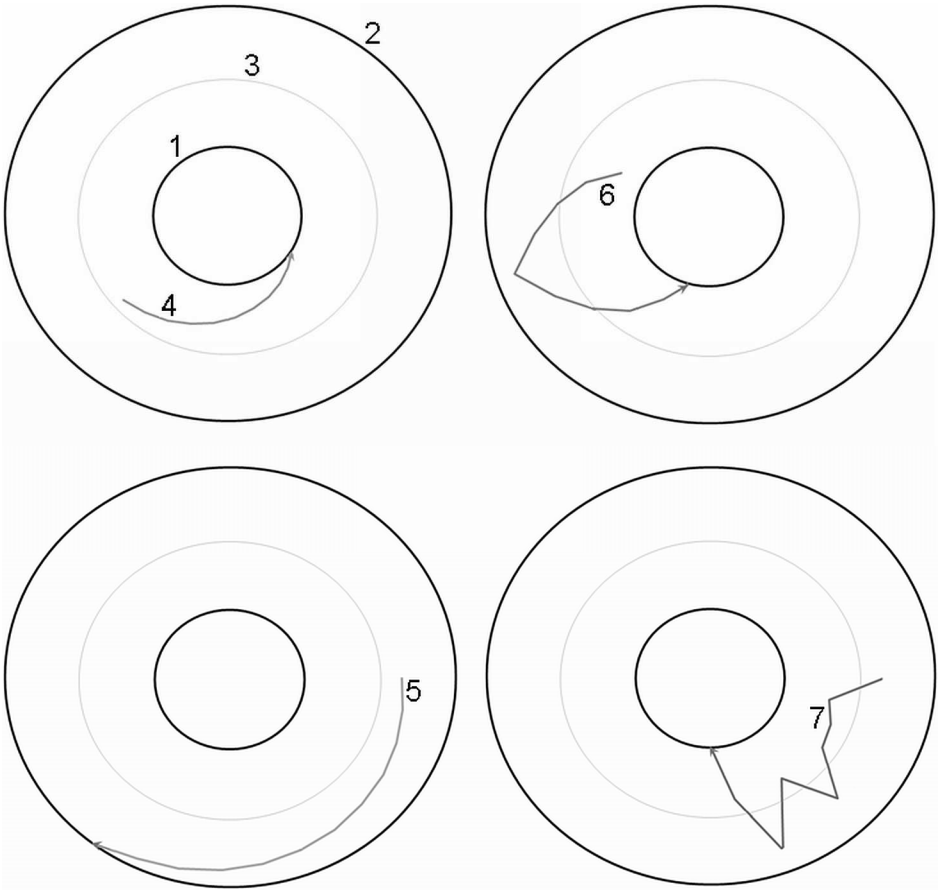

Fig. 3

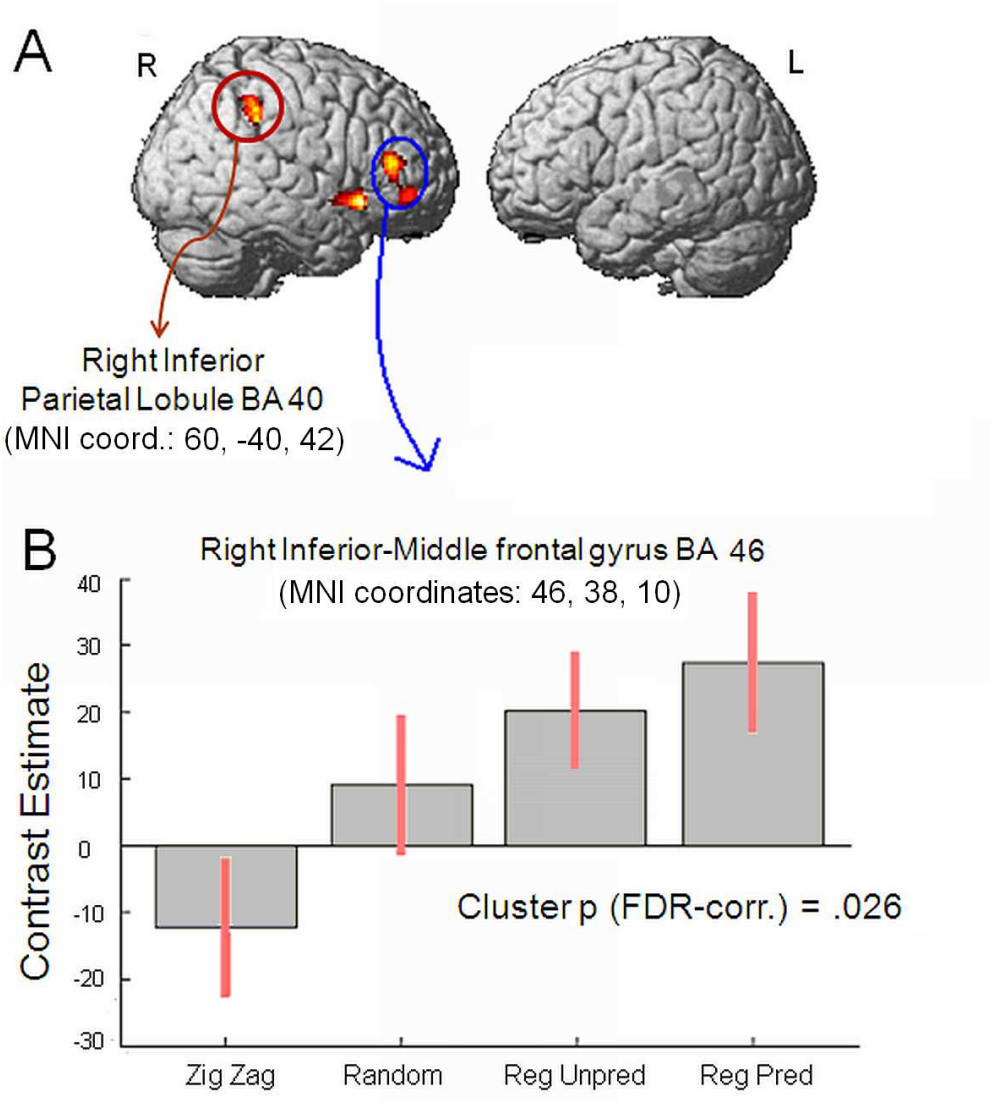
A
R
L
Right Inferior
Parietal Lobule BA 40
(MNI coord.: 60, -40, 42)
B
Right Inferior-Middle frontal gyrus BA 46
(MNI coordinates: 46, 38, 10)
Contrast Estimate
40
30
20
10
0
-10
-20
-30
Cluster p (FDR-corr.) = .026
Zig Zag
Random
Reg Unpred
Reg Pred

Fig. 4